Cell Cycle

ISSN: 1538-4101 (Print) 1551-4005 (Online) Journal homepage: www.tandfonline.com/journals/kccy20

Exploring Mechanisms of the DNA-Damage Response: p53 Pulses and their Possible Relevance to Apoptosis

Tongli Zhang, Paul Brazhnik & John J. Tyson

To cite this article: Tongli Zhang, Paul Brazhnik & John J. Tyson (2007) Exploring Mechanisms of the DNA-Damage Response: p53 Pulses and their Possible Relevance to Apoptosis, Cell Cycle, 6:1, 85-94, DOI: 10.4161/cc.6.1.3705

To link to this article: https://doi.org/10.4161/cc.6.1.3705

[Cell Cycle 6:1, 85-e10, EPUB Ahead of Print: http://www.landesbioscience.com/journals/cc/abstract.php?id=3705; 1 January 2007]; ©2007 Landes Bioscience

Analytical Report

Exploring Mechanisms of the DNA-Damage Response

p53 Pulses and their Possible Relevance to Apoptosis

Tongli Zhang
Paul Brazhnik
John J. Tyson*

Department of Biological Science; Virginia Polytechnic Institute and State University; Blacksburg, Virginia USA

*Correspondence to: John J. Tyson; Department of Biological Science, M.C. 0406, Virginia Polytechnic Institute and State University; Blacksburg, Virginia 24061 USA; Tel.: 540.231.4662; Fax: 540.231.9307; Email: tyson@vt.edu

Original manuscript submitted: 12/12/06
Manuscript accepted: 12/12/06

This manuscript has been published online, prior to printing for Cell Cycle, Volume 6, Issue 1. Definitive page numbers have not been assigned. The current citation is: Cell Cycle 2007; 6(1):
http://www.landesbioscience.com/journals/cc/abstract.php?id=3705
Once the issue is complete and page numbers have been assigned, the citation will change accordingly.

KEY WORDS

p53, stress response, apoptosis, feedback control, protein networks

ACKNOWLEDGEMENTS

This work was supported by NSF grant DMS-0342283, by DARPA grant F30602-02-0572, and by the James S. McDonnell Foundation (21002050).

NOTE

Supplemental information can be found at:
www.landesbioscience.com/supplement/zhangCC6-1-sup1.txt
www.landesbioscience.com/supplement/zhangCC6-1-sup2.txt
www.landesbioscience.com/supplement/zhangCC6-1-sup3.txt
www.landesbioscience.com/supplement/zhangCC6-1-sup4.txt
www.landesbioscience.com/supplement/zhangCC6-1-sup5.txt
www.landesbioscience.com/supplement/zhangCC6-1-sup6.txt

ABSTRACT

The transcription factor p53 plays a central role in maintaining genomic integrity. Recent experiments in MCF7 cells have shown that p53 protein level rises and falls in distinct pulses in response to DNA damage. The amplitudes of and intervals between pulses seem to be independent of the extent of damage, and some cells generate regular pulses of p53 over many days. Identifying the molecular mechanisms responsible for such interesting behavior is an important and challenging problem. This paper describes four dual-feedback mechanisms that combine both positive and negative feedback loops, which have been identified in the signaling network responsible for p53 regulation. Mathematical models of all four mechanisms are analyzed to determine if they are consistent with experimental observations and to characterize subtle differences among the possible mechanisms. In addition, a novel molecular mechanism is proposed whereby p53 pulses may induce, at first, cell cycle arrest and, if sustained, cell death. The proposal accounts for basic features of p53-mediated responses to DNA damage and suggests new experiments to probe the dynamics of p53 signaling.

INTRODUCTION

Mutations of the *p53* gene are found in more than 50% of human cancers.[1] The p53 protein is a transcription factor controlling the expression of many genes involved in cell cycle regulation, repair of DNA damage, and programmed cell death. p53 suppresses tumor genesis by guarding the genome against DNA damage that may mutate other genes more directly responsible for unrestrained cell growth and division. In undamaged cells, p53 protein level is kept low by Mdm2, a protein that promotes p53 degradation.[2] If p53 level rises too high, it induces production of more Mdm2, which drives p53 level back down.[3] However, when DNA is damaged, p53 accumulates, [4] inducing genes to block DNA synthesis, repair the damage or commit the cell to apoptosis.

In a ground-breaking study of p53 and Mdm2 protein levels in single cells of a breast cancer cell line (MCF7), Lahav et al.[5] showed that p53 and Mdm2 rise and fall in a series of pulses after DNA-damaging gamma irradiation. Although they saw at most two pulses in the 16 hours that each cell was observed, they concluded that the number of pulses increases with increasing radiation dose, while pulse amplitudes and inter-pulse intervals remain almost constant. This so-called 'digital response' was examined in more detail by the same experimental group in a recently published report[6] of p53 responses in hundreds of individual cells observed for as long as 60 hours. The rules of p53 signaling in response to DNA damage in these transformed cells are clearer now: (1) some cells exhibit regular oscillations with a period of 4–7 hours, but other cells exhibit highly irregular bursts or do not oscillate at all, (2) the proportion of cells exhibiting regular oscillations in the population increases with radiation dose, and (3) during a train of regular oscillations, pulse amplitude is more variable than inter-pulse interval. Recent observations by Hamstra et al.[7] indicate that p53 oscillations are not a peculiarity of MCF7 cells.

In the experiments of Geva-Zatorsky et al.[6] it appears that DNA damage is not completely repaired in some cells. The remaining damage triggers unrelenting pulses of p53. The fraction of cells that respond in this fashion is proportional to the intensity of the initial radiation dose. In addition, the MCF7 cells studied by these authors are deficient of caspase 3 and defective in inducing apoptosis in response to irreparable DNA damage.[8]

These unexpected and remarkable observations raise a number of questions about the generality of pulsatile p53 signaling (is it peculiar to this transformed cell line?), about the molecular mechanism of the oscillations, and about their physiological significance. In this

Table 1 **Cell lines in which the proposed interactions are observed**

Positive Feedback Effect	Cell Line and Reference
Mdm2 enhances p53 translation	H1299 cells[30]
p53 enhances C-Ha-Ras expression	Saos-2T cells[34]
JNK1 phosphorylates p53 on Ser34	293T cells [65]
MAPK phosphorylates p53 on Thr73 and Thr83	In vitro[66]
Mdm2 enhances p63 transcriptional activity	Saos2 cells[37]
Mdm2 increases p63 protein level	Cos-7 cells[37]
p63 induces *MDM2* expression	Saos-2 cells and EBC-1 cells[36]

Table 2 **Protein components of the models**

Abbreviation	Name and/or Function
p53	Transcription factor, tumor suppressor protein
Mdm2	Mouse double minute 2 homolog, cofactor for ubiquitinylation
Wip1	Wild type p53-induced phosphatase 1
p53DINP1	p53-dependent damage-inducible nuclear protein 1, kinase
PUMA	p53-upregulated modulator of apoptosis
p53AIP1	p53-regulated apoptosis-inducing protein 1
APAF1	Apoptotic protease activating factor 1
E2F1	Transcription factor
p21	Cyclin-dependent kinase inhibitor

paper we address questions two and three. Is the negative feedback loop (p53 upregulates Mdm2, which deactivates p53) sufficient to explain the observed oscillations? What roles might positive feedback play in generating and stabilizing oscillations? How might apoptosis be triggered by repeated pulses of p53 but not by only a few pulses?

The p53-Mdm2 negative feedback loop is the basis of three published models of p53 pulsatile signaling.[9-11] Although it is possible for a negative feedback loop to generate sustained oscillations, there are several problems associated with this hypothesis. First of all, negative feedback is more commonly used for homeostasis than for oscillation. Indeed, the primary function of the p53-Mdm2 negative feedback relation is probably to maintain a stable steady state of low p53 level under most conditions.[12, 13] To generate sustained oscillations, a negative feedback loop must experience a significant time delay. There are many opportunities for such delays in the processes of gene expression and molecular transport between nucleus and cytoplasm. Nonetheless, 'pure' negative feedback oscillators are not very robust. They tend to oscillate over restricted ranges of parameter values, and give birth to oscillations of small amplitude. In order to see large amplitude oscillations of p53 in their negative feedback models, Ma et al.[10] and Chickarmane et al.[11] had to introduce strong nonlinearities (ultra-sensitivity or positive feedback) into their assumptions about the DNA-damage signaling pathway (to be considered in more detail in the Discussion and Fig. 6).

These features of negative feedback oscillators were demonstrated elegantly in a set of experiments carried out recently by Pomerening et al.[14] on the periodic activation of mitosis promoting factor (MPF) in frog egg extracts. They argued that robust, large-amplitude oscillations of MPF require a combination of negative feedback and positive feedback (self-amplification). When the positive feedback loop is eliminated (by knocking out a phosphorylation site on MPF), Pomerening et al. showed that the pure negative feedback loop supports oscillations of smaller amplitude and higher frequency. Indeed, the negative feedback oscillations appear to be damping out, and their signal is so attenuated that nuclei in the extract are no longer synchronized in their mitotic state.

To create robust and reliable p53 oscillations, Ciliberto et al.[15] proposed that the p53-Mdm2 negative feedback loop be supplemented by a positive feedback loop. They suggested that p53 might amplify its own accumulation by activating PTEN, a phosphatase that inhibits Mdm2 transport into the nucleus. Because less Mdm2 gets into the nucleus, p53 degradation is attenuated and more p53 accumulates. This is a plausible mechanism, but not in MCF7 cells used in Alon's experimental group. We will show in this paper that other routes of positive feedback may contribute to the generation of p53 pulses. In particular, Mdm2 can elevate its own activator p53, Mdm2 can facilitate its own activation independent of p53, and p53 can promote its own activation without involving Mdm2. In this paper, we survey the biological evidence for these positive feedback loops (Table 1), and explore the types of pulsatile responses generated by the combined positive and negative feedback loops.

In addition, we investigate a possible function of p53 pulses. When activated, p53 has three jobs to perform: first, it arrests cell cycle progression, preventing replication of damaged DNA; second, it induces synthesis of DNA repair proteins; third, if the damage is too severe, p53 triggers programmed cell death to eliminate irreparably damaged cells. Whereas cell cycle arrest is a reversible process (cells return to normal proliferation after the damage is repaired), apoptosis is an irreversible decision. It has long been puzzling how p53 chooses between these two fates.[4, 16-21] From a plausible mechanism and mathematical model, we show that pulses of p53 can be used to distinguish between arrest/repair and cell suicide. We also propose several experiments that can refine our understanding of p53 dynamics and function.

MODELING METHODS AND ASSUMPTIONS

All models are constructed at the protein level; the protein components we use are listed in Table 2. For each model, we present a mechanism (see Fig. 1, column 1) and a set of governing kinetic equations (non-linear ordinary differential equations) (Table 3). Numerical integration of the ODEs and bifurcation analysis were carried out with XPPAUT, a software program freely downloadable from www.math.pitt.edu/~bard/xpp/xpp.html. Values for the rate constants in each mechanism (Table 4) were chosen by a trail-and-error method to give simulations and bifurcation diagrams that are consistent with known properties of p53 and Mdm2 pulses. The bifurcations and dynamics of the models are robust to small perturbations on the constants.

Our models are based on established biological facts supplemented by some assumptions and simplifications. The latter are needed because current knowledge is limited and because we want to emphasize generic mechanisms rather than mechanistic details. The following assumptions and simplifications are common to all our models.

(1) Transcriptional regulation is replaced by regulation of corresponding protein synthesis, and is incorporated where needed, using Hill functions,

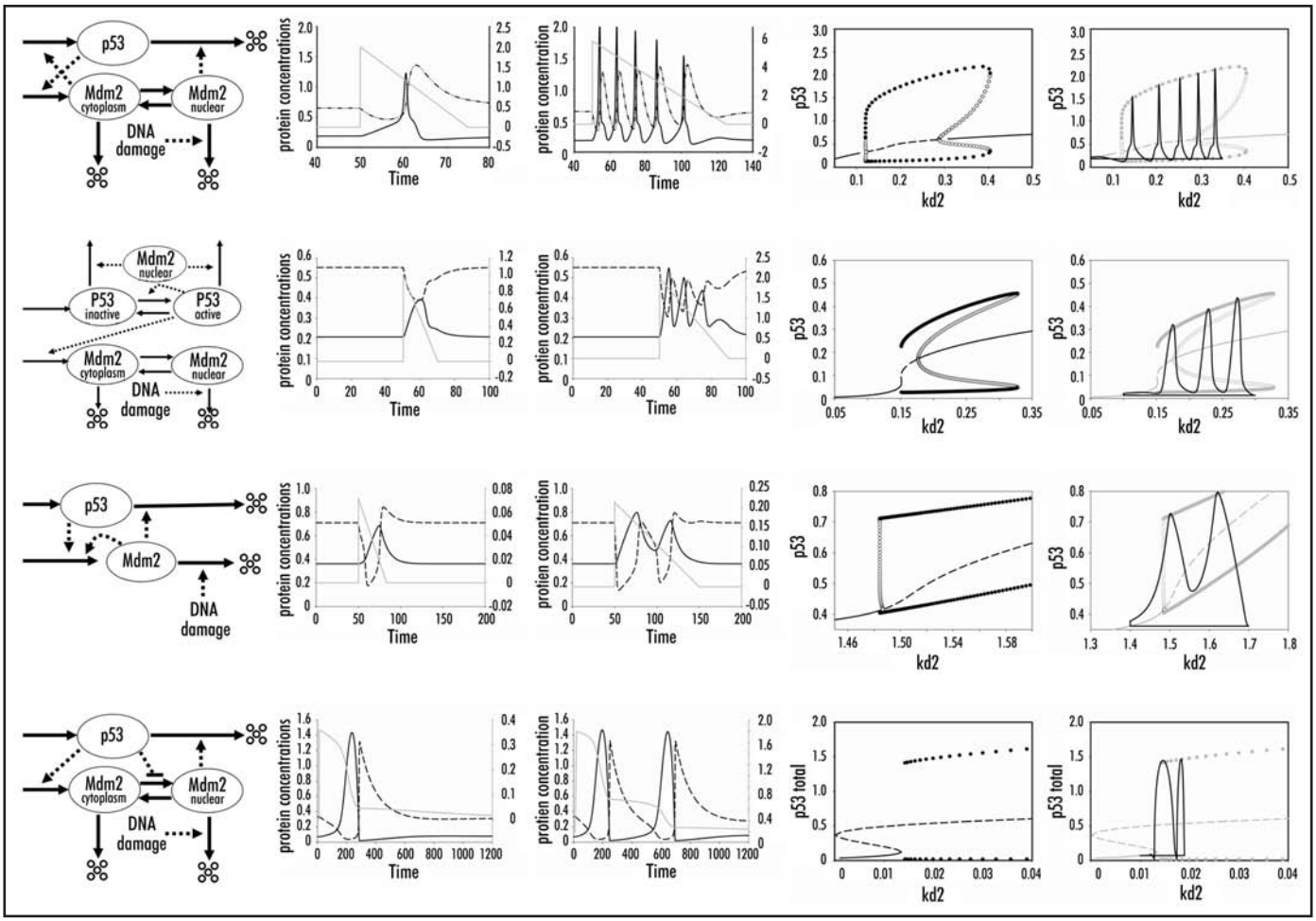

Figure 1. Four models for generating p53 pulses by a combination of positive and negative feedback loops. Row 1, Mdm2 activates p53. Row 2, p53 activates itself independently of Mdm2. Row 3, Mdm2 activates itself independently of p53. Row 4, p53 inactivates Mdm2. Column 1, wiring diagram. Column 2, response to small DNA damage; solid line = [p53]; dashed line = [nuclear Mdm2]; gray line = DNAdamage. The extent of DNA damage is indicated on the scale at the right side of the figure. Column 3, response to larger DNA damage (notations as in column 2). Column 4, bifurcation diagram. Column 5, multi-pulse response (solid line in column 3) plotted on top of bifurcation diagram (column 4). In the wiring diagrams, ovals represent proteins, solid arrows represent chemical reactions, dashed arrows represent catalytic effects of a species on a reaction, and a set of five small circles represents degradation products.

$$H(x) = \frac{x^n}{J^n + x^n}$$

to characterize the effect of a transcription factor ([TF] = x) on the rate of synthesis of the regulated protein. Each time-varying protein concentration is represented in the model rate equations by a dimensionless state variable (because the experimental data do not permit us to estimate actual concentration units). Time t is also a dimensionless variable, but appropriate units (in min or h) are easily estimated by comparing simulated pulse trains to observed ones.

(2) p53 degradation is a ubiquitin-dependent process, known to be mediated by Mdm2.[2] A complete picture of this process is quite complex. Besides p53, Mdm2 can also ubiquitinate itself, enhancing its own degradation. Auto-ubiquitination of Mdm2 is regulated by $p14^{ARF}$, a tumor suppressor protein, and by Mdm2 homologs.[22, 23] Both p53 and Mdm2 can be de-ubiquitinated by HAUSP.[24] Other factors, e.g., p300, can also affect p53 ubiquitination.[25] Without dwelling on all these details, we merely assume that Mdm2 significantly enhances p53 degradation when its nuclear concentration exceeds a certain threshold value, using a Goldbeter-Koshland function[26] to express the effect.

(3) DNA damage is known to shorten Mdm2 half-life[27] through ATM-mediated phosphorylation.[28, 29] Disregarding the details of this process, we just assume that the corresponding rate constant, k_{d2}, increases linearly with DNA damage. In those models that distinguish nuclear and cytoplasmic forms of Mdm2, only the nuclear form is destabilized by DNA damage.

(4) A detailed mechanism for DNA damage repair is not considered here. We adopt the simplest assumption that damage is repaired at a constant rate, independent on p53 and Mdm2 levels. Interested readers are referred to Ma's work, [10] where a stochastic damage repair model is used to mimic the dependence of oscillation numbers on radiation levels.

RESULTS

Models combining positive and negative feedback loops. The fundamental negative feedback loop (p53 → Mdm2 —| p53) can be supplemented by a positive feedback loop in four different ways: (1) Mdm2 activates p53; (2) p53 activates itself, independently of Mdm2; (3) Mdm2 activates itself, independently of p53; or (4) p53 inhibits Mdm2. In this section we compare the dynamics of

Table 3 **Differential equations for the models in Figure 1**

Goldbeter-Koshland Function (Goldbeter and Koshland, 1981):

$$G(u,v,q,r)=\frac{2\cdot u\cdot r}{(v-u+v\cdot q+u\cdot r+\sqrt{(v-u+v\cdot q+u\cdot r)^2-4\cdot u\cdot r\cdot(v-u)}}$$

Heaviside Function:

$$H(x)=\begin{cases}1 & \text{if } x>0\\ 0 & \text{if } x\le 0\end{cases}$$

DNA damage and degradation rate constants:

$$(1)\quad \frac{dDNAdamage}{dt}=-k_{repair}\cdot H(DNAdamage)$$

$$(2)\quad k_{d2}=k'_{d2}\cdot(1+DNAdamage)$$

$$(3)\quad k_{d53}=k'_{d53}+k^{*}_{d53}\cdot G([\text{Mdm2*}],\theta,J_1/[\text{p53*}],J_2/[\text{p53*}])$$

Model One

Equations 1, 2, 3; [Mdm2*] = [$Mdm2_{nuc}$], [p53*] = [p53]

$$(4)\quad \frac{d[\text{p53}]}{dt}=k'_{s53}+k^{*}_{s53}\cdot\frac{[Mdm2_{cyt}]^4}{J^4_{s53}+[Mdm2_{cyt}]^4}-k_{d53}\cdot[\text{p53}]$$

$$(5)\quad \frac{d[Mdm2_{cyt}]}{dt}=k'_{s2}+k^{*}_{s2}\cdot\frac{[\text{p53}]^4}{J^4_{s2}+[\text{p53}]^4}-k_i\cdot[Mdm2_{cyt}]+k_o\cdot[Mdm2_{nuc}]-k^{*}_{d2}\cdot[Mdm2_{cyt}]$$

$$(6)\quad \frac{d[Mdm2_{nuc}]}{dt}=k_i\cdot[Mdm2_{cyt}]-k_o\cdot[Mdm2_{nuc}]-k_{d2}\cdot[Mdm2_{nuc}]$$

Model Two

Equations 1, 2, 3; [Mdm2*] = [$Mdm2_{nuc}$], [p53*] = [$p53_{total}$]

$$(7)\quad [p53_{total}]=[p53_{active}]+[p53_{inactive}]$$

$$(8)\quad \frac{d[p53_{active}]}{dt}=k_{activation}\cdot[p53_{inactive}]-k_{inactivation}\cdot[p53_{active}]-k_{d53}\cdot[p53_{active}]$$

$$(9)\quad \frac{d[p53_{inactive}]}{dt}=k_{s53}-k_{activation}\cdot[p53_{inactive}]+k_{inactivation}\cdot[p53_{active}]-k_{d53}\cdot[p53_{inactive}]$$

$$(10)\quad k_{activation}=k'_{activation}+k^{*}_{activation}\cdot\frac{[p53_{active}]^3}{J^3_{activation}+[p53_{active}]^3}$$

$$(11)\quad \frac{d[Mdm2_{cyt}]}{dt}=k'_{s2}+k^{*}_{s2}\cdot\frac{[p53_{active}]^3}{J^3_{s2}+[p53_{active}]^3}-k_i\cdot[Mdm2_{cyt}]+k_o\cdot[Mdm2_{nuc}]-k^{*}_{d2}\cdot[Mdm2_{cyt}]$$

$$(12)\quad \frac{d[Mdm2_{nuc}]}{dt}=k_i\cdot[Mdm2_{cyt}]-k_o\cdot[Mdm2_{nuc}]-k_{d2}\cdot[Mdm2_{nuc}]$$

Model Three

Equations 1, 2, 3; [Mdm2*] = [Mdm2], [p53*] = [p53]

$$(13)\quad \frac{d[\text{p53}]}{dt}=k_{s53}-k_{d53}\cdot[\text{p53}]$$

$$(14)\quad \frac{d[\text{Mdm2}]}{dt}=k'_{s2}+k^{*}_{s2}\cdot[\text{p53}]+k^{**}_{s2}\cdot\frac{[\text{Mdm2}]^4}{J^4_{s2}+[\text{Mdm2}]^4}-k_{d2}\cdot[\text{Mdm2}]$$

Model Four

See Ciliberto et al. [15]

these four different control systems (see Fig. 1). Model equations and parameter values are given in Tables 3 and 4.

Model One: Mdm2 activates p53. Translation of p53 mRNA is enhanced by cytoplasmic Mdm2, according to the report of Yin et al.[30] Combined with p53-induced *MDM2* transcription, Mdm2 thereby enhances its own synthesis (Fig. 1, row 1, column 1). In absence of DNA damage (*DNA damage* = 0), p53 and Mdm2 concentrations settle on the stable steady state solution of the model (obtained by setting the right-hand sides of the ODEs to zero). Steady state concentrations (see Table 4) are used as initial conditions for all subsequent simulations. When DNA damage is introduced, degradation of nuclear Mdm2 increases, and its concentration begins to fall. The falling rate of Mdm2-dependent p53 degradation permits p53's level to rise. Increased transcriptional activation of the *MDM2* gene causes a rise in cytoplasmic Mdm2, which returns the favor by enhancing the rate of translation of p53 mRNA. This positive feedback results in abrupt increases of both p53 and cytoplasmic Mdm2. As cytoplasmic Mdm2 increases, more and more of it enters the nucleus, where it eventually promotes enough p53 degradation to drive p53 level back down. Consequently Mdm2 synthesis rate decreases, resulting in a drop of nuclear Mdm2 level. Meanwhile the initial DNA damage is being repaired at a constant rate (we assume). If the damage is repaired quickly enough, the p53-Mdm2 control system returns to the stable steady state, resulting in a single-pulse response. If sufficient DNA damage remains after the first pulse, it can force the control system to generate a second pulse, and so on. The responses to 'small' and 'large' amounts of DNA damage are illustrated in Figure 1, row 1, columns 2 and 3.

The DNA damage threshold for p53 activation can be derived from the bifurcation point where the steady state solution of the model loses stability and gives way to limit cycle oscillations (a 'Hopf' bifurcation point). The one-parameter bifurcation diagram ('signal-response' curve) for Model One is given in Figure 1, row 1, column 4. We choose as bifurcation parameter the rate constant for Mdm2 degradation in the nucleus: k_{d2} = $k'_{d2}\cdot$(*DNAdamage* + 1), where *DNAdamage* is a dimensionless number that gives the percentage increase in k_{d2} above its basal value (k_{d2}' = 0.05). (For example, *DNAdamage* = 1 means a 100% increase in the value of k_{d2}.) The steady state for Model One loses stability by a subcritical Hopf bifurcation at k_{d2} = 0.12, which corresponds to *DNAdamage_threshold* = 1.4.

In Figure 1, row 1, column 5, we plot the simulated response (Fig. 1, row 1, column 3) on top of the bifurcation diagram (Fig. 1, row 1, column 4). When DNA damage is introduced,

Table 4 **Parameter values and steady states for the models in Figure 1**

Model	Parameter Values	Steady States
One	$k'_{d53} = 0.27$, $k''_{d53} = 8.25$, $\theta = 0.83$, $k'_{d2} = 0.05$ $k'_{s53} = 0.6$, $k''_{s53} = 2.56$, $J_{s53} = 0.45$, $k'_{s2} = 0.15$ $k''_{s2} = 4.23$, $J_{s2} = 0.92$, $k_i = 0.41$, $k_o = 0.05$ $k''_{d2} = 0.79$, $k_{repair} = 0.08$, $J_1 = J_2 = 0.1$	[p53] = 0.19 $[Mdm2_{cyt}] = 0.19$ $[Mdm2_{nuc}] = 0.78$
Two	$k'_{d53} = 0.3$, $k''_{d53} = 8$, $\theta = 0.8$, $k'_{d2} = 0.1$ $k'_{s53} = 0.6$, $k_{inactivation} = 0.1$, $k_{activation} = 0.2$, $k''_{activation} = 5$ $J_{activation} = 0.2$, $k'_{s2} = 0.2$, $k''_{s2} = 3$, $J_{s2} = 0.7$ $k_i = 0.4$, $k_o = 0.05$, $k''_{d2} = 0.7$, $k_{repair} = 0.05$	$[p53_{active}] = 0.01$ $[p53_{inactive}] = 0.19$ $[Mdm2_{cyt}] = 0.21$ $[Mdm2_{nuc}] = 0.55$
Three	$k'_{d53} = 0.005$, $k''_{d53} = 0.1$, $\theta = 0.5$, $k'_{d2} = 0.4$ $k_{s53} = 0.0276$, $k'_{s2} = 0.01$, $k''_{s2} = 0.5$, $k''_{s2} = 1$, $J_{s2} = 0.5$, $k_{repair} = 0.0021429$, $J_1 = J_2 = 0.1$	[p53] = 0.36 [Mdm2] = 0.71
Four	See Ciliberto et al.[15]	

k_{d2} increases abruptly from its basal value to its checkpoint-elevated value, and then decreases linearly with time, as the DNA is repaired. The control system generates one, two, three or more pulses, until k_{d2} drops below the bifurcation point and the steady state regains stability. Since the stable limit cycle in Model One is generated by a subcritical Hopf bifurcation, the pulses are born with large amplitude, and they retain large amplitude and nearly constant period as *DNAdamage* decreases.

Model Two: p53 promotes its own activation independently of Mdm2. Phosphorylation of p53 can enhance its activity as a transcription factor.[31-33] The signal transduction protein c-Ha-Ras can enhance p53 phosphorylation through JNK, MAPK and PKC, and c-Ha-Ras gene expression is itself positively regulated by p53.[34] Thus, p53 can promote its own activation by this positive feedback loop (Fig. 1, row 2, column 1). (To keep the model simple, c-Ha-Ras is not considered explicitly.) For ODEs and parameter values, see Tables 3 and 4. Typical simulations for 'small' and 'large' DNA damage are shown in Figure 1, row 2, columns 2 and 3. As for Model One, a verbal description of the sequence of events during the simulated response is easily given. More instructive is the bifurcation diagram of Model Two (Fig. 1, row 2, column 4), which demonstrates that oscillations in this model arise from a SNIC ('saddle-node invariant circle') bifurcation, [35] rather than a subcritical Hopf bifurcation, as in Model One. Nonetheless, the characteristics of the p53 time courses (Fig. 1, rows 1 and 2, column 5) are quite similar: as k_{d2} falls back to normal, there is a slight decrease in oscillation amplitude and a slight increase in inter-pulse intervals. Due to the typical noise levels in p53 measurements, these slight changes would be difficult to observe experimentally, but they may be reflected in the fact that p53 pulse amplitudes are more variable than inter-pulse intervals.[6]

In both Models One and Two, if DNA damage is too large ($k_{d2} > 0.4$), then p53 pulses cease and p53 concentration stays at a high steady state level. In the experiments of Hamstra et al.,[7] amplification of DNA damage elevates p53 level and dampens oscillations.

Model Three: Mdm2 activates itself independently of p53. Transcription of the *MDM2* gene can be induced by the p53-homolog, p63, [36] and Mdm2 can in turn increase the level of and transcriptional activity of p63 protein.[37] These effects create the possibility for Mdm2 to activate itself via a p53-independent pathway. Combining this positive feedback with the p53-Mdm2 negative feedback, we create Model Three in Figure 1, row 3, column 1. To keep the model simple, we do not represent p63 explicitly, but just assume that there is a threshold above which Mdm2 enhances its own synthesis. Figure 1, row 3, columns 2 and 3 show, for Model Three, its response to 'small' and 'large' amounts of DNA damage, and Figure 1, row 3, columns 4 and 5 show that p53 pulses in Model Three arise from a subcritical Hopf bifurcation.

Model Four: p53 inhibits Mdm2. There is the fourth possibility, that p53 inhibits the action of Mdm2 by down-regulating Mdm2 transport into the nucleus (Fig. 1, row 4, column 1); this is the case studied previously by Ciliberto et al. (2004). ODEs, parameter values, simulations (Fig. 1, row 4, column 2 and 3) and bifurcation diagrams are presented as for Models One-Three. Model Four generates p53 pulses by a SNIC bifurcation (Fig. 1, row 4, column 4 and 5).

How p53 pulses might determine cell fate? In the preceding section we studied four plausible mechanisms that combine positive and negative feedback loops to generate robust pulses of p53 and Mdm2 in response to DNA damage. When the damage is repaired, the pulses cease. If the damage is not repaired, the pulses persist, and it is reasonable to suppose that sustained p53 pulsing is the signal for triggering programmed cell death. In this section we propose a mechanism (Fig. 2) whereby p53 pulses might coordinate cell cycle arrest and apoptosis. Converting the mechanism into a quantitative model, we show how multiple pulses of p53 might trigger apoptosis whereas a few pulses do not.

p53 is a transcription factor that upregulates a broad range of target genes.[38-47] Cell types, stimulation signals, cofactors, and post-translational modifications can affect p53 stability and target preference.[17, 48-50] For example, human p53 has 17 phosphorylation sites, which play important roles in regulating p53 functions, [31-33, 48]and Ser46 phosphorylation, in particular, is closely linked with induction of apoptotic genes.[44] In our simplified model, we define three forms of p53: p53-killer, p53-helper and p53-lurker. We assume these different p53 forms are modified differently and induce different target genes.

We assume that p53-killer activates apoptotic genes like *PUMA, p53DINP1* and *p53AIP1*. PUMA protein induces release of cytochrome c (cytoC) from mitocondria, [47] which stimulates the APAF1 protein complex to activate caspase 9, which in turn activates 'executioner caspases' that carry out the cell-death program. Caspase 9 activation occurs via apoptosomes.[51] We assume that pro-caspase 9 is always available, and apoptosomes form when both APAF1 and cytoC are present. The *APAF1* gene has binding sites for both p53 and E2F1.[52, 53] We assume that p53-killer and E2F1 are both necessary to induce APAF1 protein production efficiently. p53 phosphorylation on Ser46 is enhanced by p53DINP1[44] and inhibited by the serine/threonine phosphatase Wip1, although Wip1 does not directly dephosphorylate p53 on Ser46.[54] We assume that the phosphorylation of p53 on Ser46 depends on the concentrations of these two enzymes: if there is more p53DINP1 than Wip1, p53 is preferentially phosphorylated on Ser46 and converted to the killer form.

Another p53 form is called 'p53-helper' for three reasons. (1) We assume this form of p53 prefers to induce p21, which in turn induces cell cycle arrest, [55] giving the cell time to repair the damaged DNA. (2) By blocking CDK activity, p21 indirectly activates the retino-

blastoma protein, which binds to and inhibits E2F1, [18] thereby blocking APAF1 expression. (3) We assume that the helper form of p53 induces Wip1, which, as mentioned above, inhibits Ser46 phosphorylation[54] and thus blocks formation of the killer form of p53. What's more, we assume p53 helper is further modified by some of its target genes. We are aware that p21 potentially regulates p53 through several different pathways, [13, 56] but these feedback effects are not considered in our current model.

The third form of p53 is called 'p53-lurker' because it can be transformed into p53-killer by the action of p53DINP1, and we assume that p53-lurker contributes to the induction of p53DINP1.

The wiring diagram in Figure 2 is translated into ODEs presented in Table 5, along with suggested parameter values (Table 6). The apoptosis-specific equations (Table 5) are combined with ODEs of Model One (Table 3). The DNA-damage-induced pulses of total p53 that are generated by Model One are interpreted by the apoptosis model to determine if and when apoptosis should occur. In absence of DNA damage, the combined system reaches a stable steady state (Tables 4 and 6) and all simulations are started from this state.

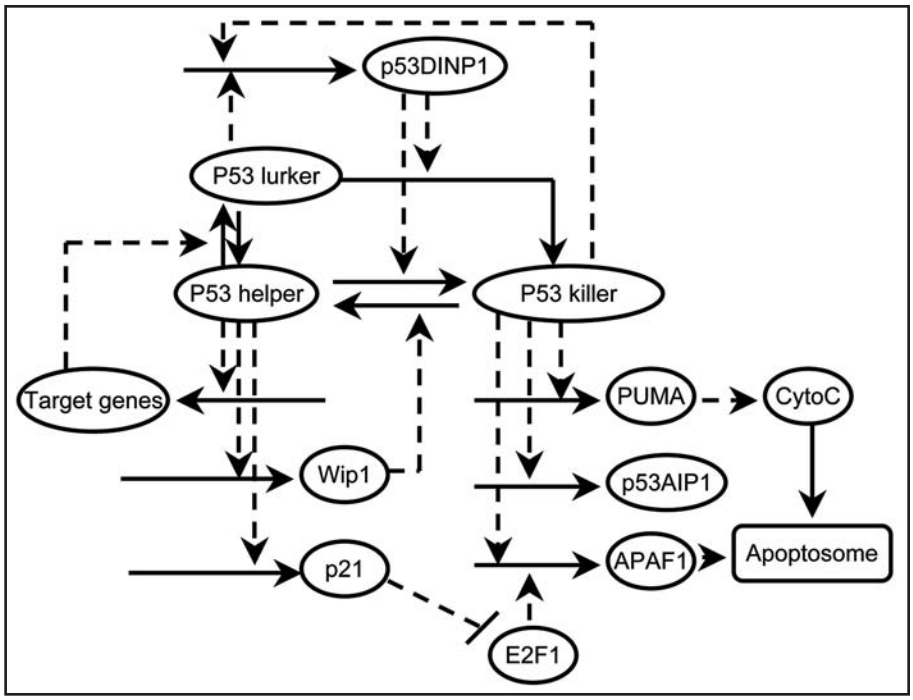

Figure 2. Wiring diagram of apoptosis model (notations as in Fig. 1).

After DNA is damaged, p53 accumulates in pulses with its distribution between different forms depending on time and the number of pulses (Fig. 3A). Initially, the p53-helper-induced phosphatase Wip1 exceeds the p53-lurker-induced kinase p53DINP1, and so the p53 pulses consist mainly of 'helpers' and 'lurkers'. Later, as Wip1 decreases and p53DINP1 increases, due to the transformation of p53-helper into p53-lurker, p53-killer starts to accumulate. These transformations link the extent of DNA damage with cell fate. If the damage is quickly fixed, only p53-helper and lurker forms appear, apoptotic genes are not activated, and cells can recover after a transient arrest. Sustained DNA damage induces accumulation of p53-killer and subsequent apoptosis. Model simulations also display how different p53 target genes are induced at different times after DNA damage (Fig. 3B). In particular, p21 and Wip1 are expressed in our model earlier than p53DINP1 and p53AIP1, the simulation results correctly describing the experimentally observed facts.[39, 43, 44]

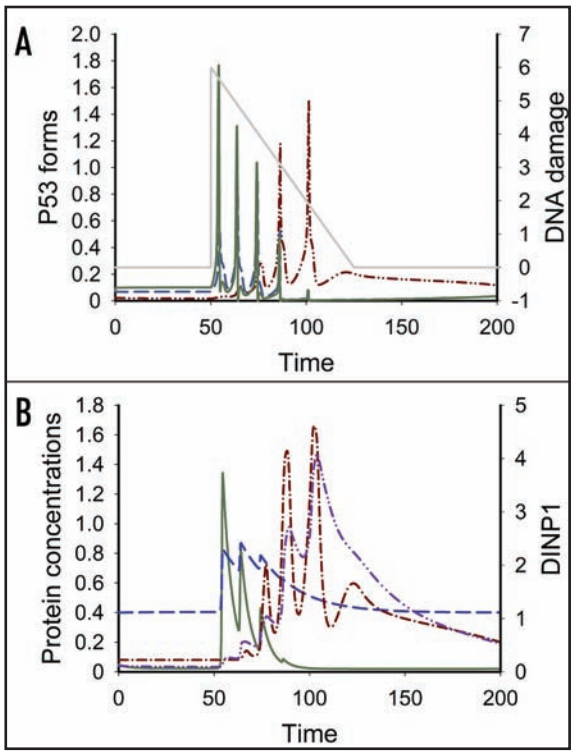

Figure 3. Response of apoptosis model to *DNAdamage* = 6. (A) p53 forms: solid line (green) = [p53 helper], dashed line (blue) = [p53 lurker], dash-dot line (red) = [p53 killer], gray = *DNAdamage*. (B) p53 target genes: solid line (green) = [p21], dashed line (blue) = [Wip1], dash-dot (red) = [p53AIP1], dash-dot-dot (purple) = [p53DINP1].

Mutations of the control system can easily change cell fates from the wild-type response. Although small damage (e.g., corresponding in our model to *DNAdamage* = 4) does not induce apoptosis in wild-type cells, it can induce apoptosis if Wip1 is knocked out or if p53DINP1 is over-expressed. On the other hand, larger damage (e.g., *DNAdamage* = 6) induces apoptosis in wild-type cells but will not induce apoptosis when p21 or Wip1 is overexpressed. Our simulation results are summarized in Table 7.

To demonstrate how Wip1 affects the balance between different p53 forms, we hold total p53 constant and compute the bifurcation diagram for Wip1 (presented in Fig. 4). The diagram shows that for certain value of Wip1, the balance can exhibit bistability, there can be either high p53 killer and low helper/lurker or the opposite. Furthermore, this bistability depends on the level of total p53. It is lost when total p53 is too high or too low (Fig. 4B).

Table 5 **Differential equations for the model in Figure 2**

$$(1)\quad \frac{d[p53_{killer}]}{dt} = [DINP1]\cdot\frac{[p53_{nonkiller}]}{0.1+[p53_{nonkiller}]} - [Wip1]\cdot\frac{[p53_{killer}]}{0.1+[p53_{killer}]}$$

$$(2)\quad [p53_{nonkiller}] = [p53] - [p53_{killer}]$$

$$(3)\quad \frac{d[p53_{lurker}]}{dt} = k_{TGp53}\cdot[TG]\cdot\frac{[p53_{helper}]}{0.1+[p53_{helper}]} - \theta_{TG}\cdot\frac{[p53_{lurker}]}{0.1+[p53_{lurker}]}$$

$$(4)\quad [p53_{helper}] = [p53_{nonkiller}] - [p53_{lurker}]$$

$$(5)\quad \frac{d[TG]}{dt} = k'_{sTG} + k''_{sTG}\cdot\frac{[p53_{helper}]^3}{J^3_{sTG}+[p53_{helper}]^3} - k_{dTG}\cdot[TG]$$

$$(6)\quad \frac{d[Wip1]}{dt} = k'_{sWip1} + k''_{sWip1}\cdot\frac{[p53_{helper}]^3}{J^3_{sWip1}+[p53_{helper}]^3} - k_{dWip1}\cdot[Wip1]$$

$$(7)\quad \frac{d[p21]}{dt} = k'_{sp21} + k''_{sp21}\cdot\frac{[p53_{helper}]^3}{J^3_{sp21}+[p53_{helper}]^3} - k_{dp21}\cdot[p21]$$

$$(8)\quad \frac{d[DINP1]}{dt} = k'_{sDINP1} + k''_{sDINP1}\cdot\frac{[p53_{lurker}]^3}{J^3_{sDINP1lurker}+[p53_{lurker}]^3} + k''_{sDINP1}\cdot\frac{[p53_{killer}]^3}{J^3_{sDINP1killer}+[p53_{killer}]^3} - k_{dDINP1}\cdot[DINP1]$$

$$(9)\quad \frac{d[PUMA]}{dt} = k'_{sPUMA} + k''_{sPUMA}\cdot\frac{[p53_{killer}]^3}{J^3_{sPUMA}+[p53_{killer}]^3} - k_{dPUMA}\cdot[PUMA]$$

$$(10)\quad \frac{d[p53AIP1]}{dt} = k'_{sp53AIP1} + k''_{sp53AIP1}\cdot\frac{[p53_{killer}]^3}{J^3_{sp53AIP1}+[p53_{killer}]^3} - k_{dp53AIP1}\cdot[p53AIP1]$$

$$(11)\quad \frac{d[APAF1]}{dt} = k'_{sAPAF1} + k''_{sAPAF1}\cdot\frac{[p53_{killer}]^3}{J_{p53killer}{}^3+[p53_{killer}]^3}\cdot\frac{[E2F1]^3}{J_{E2F1}{}^3+[E2F1]^3} - k_{dAPAF1}\cdot[APAF1]$$

$$(12)\quad [E2F1] = G(\theta_{p21},\ [p21],\ 0.1,\ 0.1)$$

$$(13)\quad [cytoc] = G([PUMA],\ \theta_{PUMA},\ 0.1,\ 0.1)$$

$$(14)\quad [Apoptosome] = H([APAF1]-\theta_{APAF1})*H([cytoc]-\theta_{cytoc})$$

Goldbeter-Koshland function, $G(u, v, g, r)$, and Heaviside function $H(x)$, are defined as in Table 3.

Table 6 **Parameter values and steady states for the model in Figure 2**

Parameter Values	Steady States
k_{TGp53} = 3, θ_{TG} = 1.5, k'_{sTG} = 0.004, k''_{sTG} = 0.5	$[p53_{killer}]$ = 0.02
J_{sTG} = 1.7, k_{dTG} = 0.01, k'_{sWip1} = 0.02, k''_{sWip1} = 1.2	$[p53_{lurker}]$ = 0.08
J_{sWip1} = 1.8, k_{dWip1}= 0.2, k'_{sp21} = 0.004, k''_{sp21} = 5	[TG] = 0.41
J_{sp21} = 2, k_{dp21}= 0.2, k'_{sDINP1} = 0.004, k''_{sDINP1} = 0.5	[Wip1] = 0.40
$J_{sDINP1lurker}$ = 0.7, k'''_{sDINP1}= 1, $J_{sDINP1killer}$ = 0.5, k_{dDINP1} = 0.05	[p21] = 0.05
k'_{sPUMA} = 0.04, k''_{sPUMA} = 1, J_{sPUMA} = 0.3, k_{dPUMA} = 0.5	[DINP1] = 0.11
$k'_{sp53AIP1}$ = 0.04, $k''_{sp53AIP1}$ = 1, $J_{sp53AIP1}$ = 0.3, $k_{dp53AIP1}$ = 0.5	[PUMA] = 0.08
k'_{sAPAF1} = 0.04, k''_{sAPAF1} = 2, $J_{p53killer}$ = 0.3, J_{E2F1} = 0.3	[p53AIP1] = 0.08
k'_{dAPAF1} = 0.5, θ_{p21} = 0.5, θ_{PUMA} = 0.5, θ_{APAF1} = 0.5	[APAF1] = 0.08
θ_{cytoc} = 0.5	
k_{TGp53} = 3, θ_{TG} = 1.5, k'_{sTG} = 0.004, k''_{sTG} = 0.5	

When DNA is damaged, p53 accumulates and changes the intracellular context through gene induction, allowing the p53 control system to 'remember' the damage. We illustrate this memory effect by applying a small radiation dose (*DNAdamage* = 4.4) at t = 50, and then a second identical dose at different times after the first (Fig. 5). Two small doses given in sequence will induce apoptosis if the inter-dose interval is below a certain threshold (Δt = 181 in this case). Although our model is too speculative to give quantitatively accurate predictions, we believe it points the way to an interesting experimental test of the memory effect. Two small radiation doses, neither one of which is sufficient to induce apoptosis by itself, may combine to induce an apoptotic response, but only if the doses are given close enough together. A quantitative experimental measurement of the relationship between dose level and inter-dose interval might provide strong constraints on proposed quantitative models of the p53 pulsatile response.

DISCUSSION

The observed pulses of p53 accumulation in breast cancer cells after DNA damage by gamma radiation pose interesting challenges to experimentalists and modelers alike. From a theoretical perspective, [57] it seems obvious that in undamaged cells the p53 control system is attracted to a stable steady state with low p53 level, while DNA damage pushes the system into a regime of stable limit cycle oscillations. As the damage is repaired, the control system presumably returns to the regime of the stable steady state. The two regimes are separated by a point of 'bifurcation', where the stable steady state is supplanted by stable oscillations. There are only a few qualitatively different ways that a stable steady state gives way to stable oscillations (see, e.g., ref. 58), most notably by a Hopf bifurcation (supercritical or subcritical) or by a SNIC bifurcation (saddle-node on an invariant circle). Which type of bifurcation comes into play in this circumstance is an important theoretical question: the period and amplitude of oscillations depend strongly on the type of bifurcation, and these properties may have significant physiological consequences.

The p53-Mdm2 control system is clearly characterized by a negative feedback loop (p53 drives synthesis of Mdm2, which in turn degrades p53) which may be sufficient to generate sustained oscillation by a supercritical Hopf bifurcation, if the loop has a sufficiently nonlinear response function and sufficiently long time delays.[10, 11] In this work, as well as in the paper by Ciliberto, [15] we supplement the negative feedback loop with plausible positive feedback loops in order to generate oscillations by subcritical Hopf or SNIC bifurcations. The main differences between these two sorts of models are illustrated in Figure 6. In p53-Mdm2 models with supercritical Hopf bifurcations, the onset of oscillations is 'soft' (i.e., small amplitude). In order to get a robust oscillatory response to DNA damage of varying strengths, the authors[10,11] introduce a non-linear dependence between DNA damage level and the bifurcation parameter in their models ('ATM' activity). As DNA damage increases and decreases, the bifurcation parameter jumps abruptly between values associated with the stable steady state and values associated with robust oscillations (Fig. 6A and B). By contrast, in our models with subcritical Hopf and SNIC bifurcations, the onset of oscillations is 'hard' (i.e., the oscillations, when they first appear, have large amplitude and are robust to variations of damage level). In these cases, we need

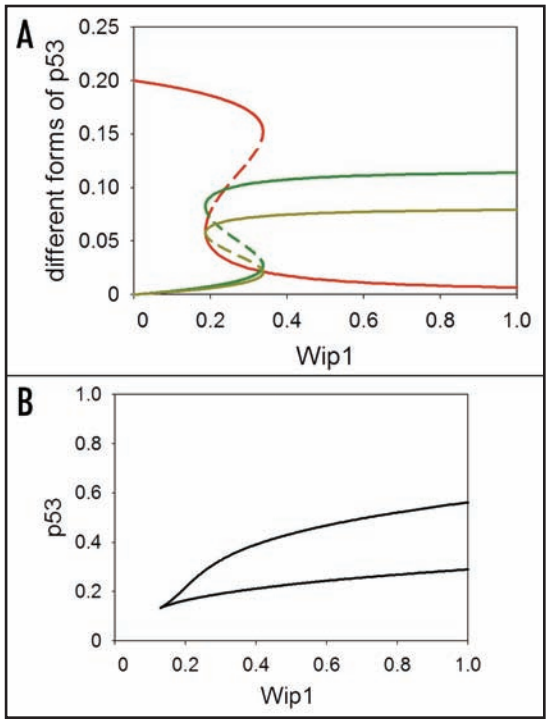

Figure 4. Bifurcation diagrams of the apoptosis model. (A) One parameter bifurcation diagram for Wip1, with $[p53_{total}] = 0.2$. Red, green and yellow lines represent p53 killer, helper and lurker, respectively. Solid (dashed) lines represent stable (resp., unstable) steady states. (B) Two parameter bifurcation diagram for Wip1 and total p53.

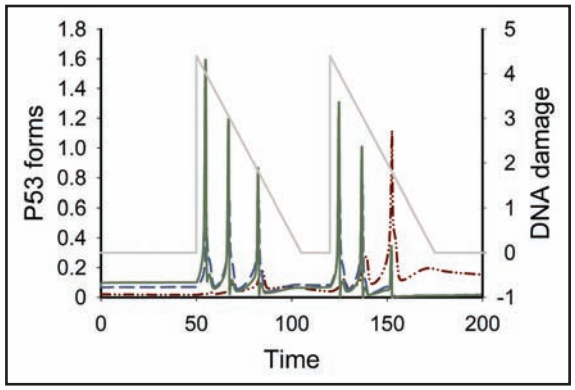

Figure 5. Response of the apoptosis model to two sequential small radiation doses. p53-killer is formed. Solid line (green) = [p53 helper], dashed line (blue) = [p53 lurker], dash-dot line (red) = [p53 killer], gray = *DNAdamage*.

only assume a simple linear dependence between damage level and bifurcation parameter (k_{d2}), see (Figs. 6C and D).

If there is non-linearity in the response of ATM to DNA damage, it may be sigmoidal (∫-shaped, as in Fig. 6A) or bistable (S-shaped, as in Fig. 6B). For the bistable case, intermediate levels of DNA damage may lead to either the stable steady state or the stable oscillatory state, depending on whether the bifurcation parameter is increasing or decreasing. The same is true for the case of a subcritical Hopf bifurcation (Fig. 6C), even if the k_{d2}-damage relationship is linear. In the other two cases (Fig. 6A and D), the coexistence of stable steady states and stable oscillations of p53 are not observed. If coexistence is indeed observed, further experiments can be carried out to determine whether bistability is generated by the ATM response pathway or by the p53-Mdm2 control loop. In either case, bistability will be attributed to a positive feedback loop, either in ATM response pathway or in the p53-Mdm2 control loop. If these presumptive loops can be knocked out by suitable mutations, it should be possible to determine which loop is necessary for the bistable response.

If no coexistence is observed for intermediate DNA damage level, further distinctions can be made by observing the p53 oscillation amplitude and period. In the case of a supercritical Hopf bifurcation (Fig. 6A), oscillations close to the bifurcation point have small and highly variable amplitude but finite and slightly variable frequency. In the case of a SNIC bifurcation (Fig. 6D), oscillations close to the bifurcation point have small and highly variable frequency but finite and slightly variable amplitude. Some evidence along these lines in the recent experiments of Geva-Zatorsky et al.[6] seems to favor the supercritical Hopf scenario.[58]

In principle, Models Two and Three can be distinguished with *MDM2*-null and *p53*-null cell lines. Model Two predicts hysteresis of active p53 in *MDM2*-null cells, while Model Three predicts hysteresis of Mdm2 level in *p53*-null cells. Ciliberto[15] suggested similar experiments, and experimental protocols for hysteresis detection can be found in Sha's work.[59]

These types of experiments may help to clarify the mechanisms generating p53 pulses. It is likely that more than one mechanism may contribute to pulsatile signaling, [56] and different mechanisms may work in different cell types. For example, even though PTEN is hardly induced by p53 in MCF-7 cells, [60] p53 may inhibit Mdm2 through Rb, [56] which is an alternative pathway for the positive feedback studied by Ciliberto.[15] The purpose of current models is to clarify certain mechanistic possibilities and to suggest alternative ways of thinking about p53 signaling in response to DNA damage. More biological information should be integrated into mathematical models to deal with such complexity and diversity of cellular regulatory systems.

In our model of apoptosis (Fig. 2), we propose a mechanism by which cell fate ('repair and survive' or 'give up and die') might

Table 7 **Context dependent effects of DNA damage**

Genotype	Parameter settings	DNA damage = 4 (small)	DNA damage = 6 (large)	Notes
Wild type	Basal parameter set	No apoptosis	Apoptosis	
p21-OP	$k'_{sp21} = 0.2$	No apoptosis	No apoptosis	a
WIP1-OP	$k'_{swip1} = 0.2$	No apoptosis	No apoptosis	b
WIP1-Δ	$k'_{swip1} = 0$; $k''_{swip1} = 0$	Apoptosis	Apoptosis	c
p53DINP1-OP	$k'_{sdinp1} = 0.01$; $k''_{sdinp1} = 2$; $k''_{sdinp1} = 4$	Apoptosis	Apoptosis	d

OP = overproduction, Δ = deletion. [a]In Bissonnette and Hunting, [67] the authors used mimosine to induce p21 and found that p21 overexpression protected cells from apoptosis after UV irradiation. [b]In Li et al, [68] the authors found that *WIP1* over-expression attenuated apoptosis induced by serum starvation. Our model is consistent with this observation.[c]*WIP1* is known as an oncogene, and *WIP1* deletion is related to tumor suppression.[69] We speculate that *WIP1* deletion may increase the cell's sensitivity to radiation-induced apoptosis. [d]In Okamura et al, [44] the authors found the coover-expression of p53 and p53DINP1 increased the cell's sensitivity to radiation-induced apoptosis.

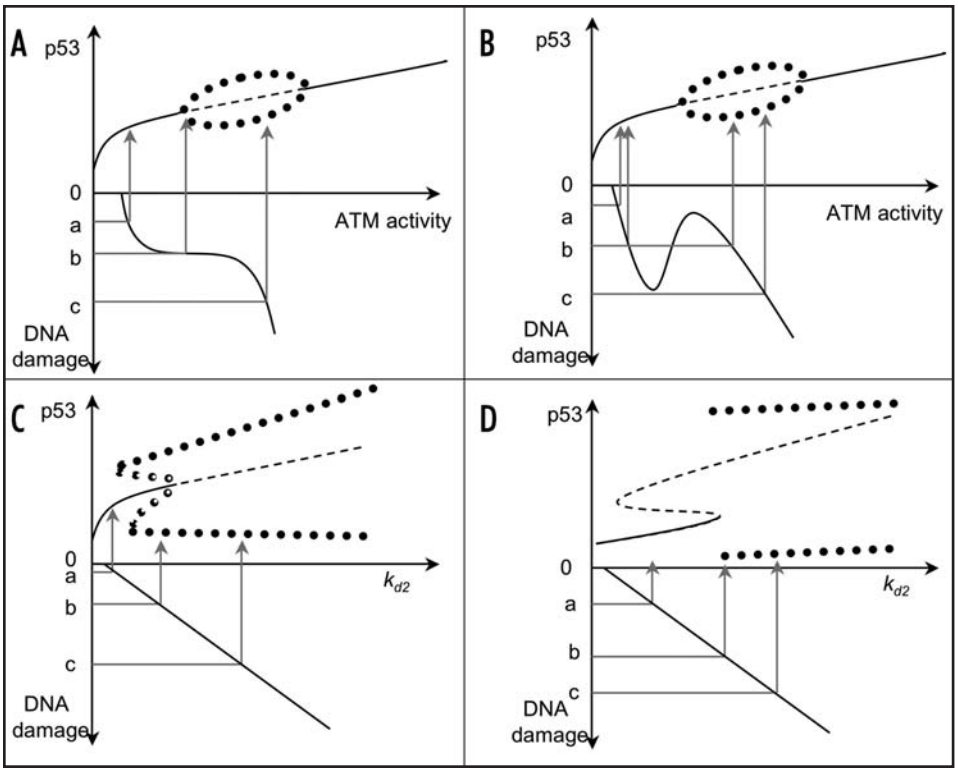

Figure 6. Schematic comparison of published models. (A) Supercritical Hopf bifurcation combined with the ATM sigmoidal switch, as in Ma et al.[10] (B) Supercritical Hopf bifurcation combined with the ATM bistable switch, as in Chickarmane et al.[11] (C) Subcritical Hopf bifurcation, as in Models One and Three in (Fig. 1). (D) SNIC bifurcation, as in Models Two and Four in (Fig. 1). In each panel we plot two curves: the upper curve is a bifurcation diagram, [p53] versus a damage signal (ATM activity, or rate constant for Mdm2 degradation); the lower curve is the dependence of the damage signal on the DNA damage level. The gray lines labeled a, b, c denote low, medium and high amounts of DNA damage. In the bifurcation diagrams, solid lines = stable steady states, dashed lines = unstable steady states, solid circles = maximum and minimum values of [p53] on a stable limit cycle, and open circles = maximum and minimum values of [p53] on an unstable limit cycle.

be determined by counting the number of p53 pulses (a 'digital' response mechanism). Alternatively, the decision might be an 'analog' response: no damage ⇒ low level of p53 ⇒ no arrest; moderate damage ⇒ moderate level of p53 ⇒ arrest and repair; large damage ⇒ high level of p53 ⇒ apoptosis. In our opinion, the digital response mode has several advantages over the analog mode:

• The analog mode is risky. Local p53 concentration may fluctuate at random to a high level that in the analog mode would induce irreversible apoptosis. By contrast, the digital mode is safe because, in the initial stage, p53-helper induces p21 and Wip1 to prevent apoptosis.

• The analog model is inconsistent. One role of p53 is to activate DNA damage repair, so high p53 concentration should mean high repair potential. It seems inconsistent to kill these cells just because their p53 concentration is high. The digital mode resolves this inconsistency. Apoptosis is induced by sustained DNA damage, not by transient high p53 concentration.

• The analog mode can be dangerous. Cells suffering from sustained small DNA damage would not commit suicide but try to stay arrested in the cell cycle. But cell cycle arrests are rarely tight; cells tend to 'adapt' to the arrest signal after some time and proceed to the next stage of the cell cycle.[61] In this case the damaged DNA will be transmitted to the next generation. The digital mode is efficient and strict. If the DNA damage is not fixed after several pulses, p53-killer induces apoptosis, ensuring the fidelity of the genome.

Our model, which emphasizes that both p53 concentration and p53 phosphorylation state are important for cell fate, is consistent with many interesting experimental observations (Table 6). Further experimental characterization of this phenomenon will be needed to pin down the mechanism of p53 pulse generation and the significance of pulses in determining cell fate after DNA damage.

Many improvements can be made to the model proposed here. Only elementary combinations of one positive and one negative feedback loop are considered in these models, but p53 appears to be regulated by lots of positive and negative feedback loops, [56, 62] which may be working simultaneously. Also, only three differently modified forms of p53 are considered in our apoptosis model, while human p53 protein has 17 phosphorylation sites[48] and phosphorylation alone can generate 2^{17} different forms of p53 proteins. Besides, our current model focuses on p53's role in transcription activation, while it is important to remember that p53 promotes apoptosis through multiple mechanisms, including transactivation, transrepression as well as direct mitochondria targeting.[21, 63, 64] Certainly, more complex models will be needed soon to accommodate the complexity of the p53 response to DNA damage.

References

1. Vogelstein B, Lane D, Levine AJ. Surfing the p53 network. Nature 2000; 408:307-10.
2. Haupt Y, Maya R, Kazaz A, Oren M. Mdm2 promotes the rapid degradation of p53. Nature 1997; 387:296-9.
3. Barak Y, Juven T, Haffner R, Oren M. mdm2 expression is induced by wild type p53 activity. EMBO J 1993; 12:461-8.
4. Meek DW. The p53 response to DNA damage. DNA Repair (Amst) 2004; 3:1049-56.
5. Lahav G, Rosenfeld N, Sigal A, Geva-Zatorsky N, Levine AJ, Elowitz MB, Alon U. Dynamics of the p53-Mdm2 feedback loop in individual cells. Nat Genet 2004; 36:147-50.
6. Geva-Zatorsky N, Rosenfeld N, Itzkoviz S, Milo R, Sigal A, Dekel E, Yarnitzky T, Polak P, Lahav G, Alon U. Oscillations and variability in the p53 system. Mol Syst Biol. 2006; 2:2006.0033.
7. Hamstra DA, Bhojani MS, Griffin LB, Laxman B, Ross BD, Rehemtulla A. Real-time evaluation of p53 oscillatory behavior in vivo using bioluminescent imaging. Cancer Res 2006; 66:7482-9.
8. Blanc C, Deveraux QL, Krajewski S, Janicke RU, Porter AG, Reed JC, Jaggi R, Marti A. Caspase-3 is essential for procaspase-9 processing and cisplatin-induced apoptosis of MCF-7 breast cancer cells. Cancer Res 2000; 60:4386-90.
9. Lev Bar-Or R, Maya R, Segel LA, Alon U, Levine AJ, Oren M. Generation of oscillations by the p53-Mdm2 feedback loop: A theoretical and experimental study. Proc Natl Acad Sci USA 2000; 97:11250-5.
10. Ma L, Wagner J, Rice JJ, Hu W, Levine AJ, Stolovitzky GA. A plausible model for the digital response of p53 to DNA damage. Proc Natl Acad Sci USA 2005; 102:14266-71.

11. Chickarmane VA, Nadim Animesh, Ray Herbert, M Sauro. A p53 oscillator model of DNA break repair control. 2005, (http://arxivorg/abs/q-bioMN/051000).
12. Blagosklonny MV. Loss of function and p53 protein stabilization. Oncogene 1997; 15:1889-93.
13. Blagosklonny MV, Demidenko ZN, Fojo T. Inhibition of transcription results in accumulation of Wt p53 followed by delayed outburst of p53-inducible proteins: p53 as a sensor of transcriptional integrity. Cell Cycle 2002; 1:67-74.
14. Pomerening JR, Kim SY, Ferrell Jr JE. Systems-level dissection of the cell-cycle oscillator: Bypassing positive feedback produces damped oscillations. Cell 2005; 122:565-78.
15. Ciliberto A, Novak B, Tyson JJ. Steady states and oscillations in the p53/Mdm2 network. Cell Cycle 2005; 4:488-93.
16. Vousden KH, Lu X. Live or let die: The cell's response to p53. Nat Rev Cancer 2002; 2:594-604.
17. Sionov RV, Haupt Y. The cellular response to p53: The decision between life and death. Oncogene 1999; 18:6145-57.
18. Pietenpol JA, Stewart ZA. Cell cycle checkpoint signaling: Cell cycle arrest versus apoptosis. Toxicology 2002; 181-182:475-81.
19. Oren M. Decision making by p53: Life, death and cancer. Cell Death Differ 2003; 10:431-42.
20. Michalak E, Villunger A, Erlacher M, Strasser A. Death squads enlisted by the tumour suppressor *p53*. Biochem Biophys Res Commun 2005; 331:786-98.
21. Haupt S, Berger M, Goldberg Z, Haupt Y. Apoptosis - The p53 network. J Cell Sci 2003; 116:4077-85.
22. Xirodimas D, Saville MK, Edling C, Lane DP, Lain S. Different effects of p14ARF on the levels of ubiquitinated p53 and Mdm2 in vivo. Oncogene 2001; 20:4972-83.
23. Stad R, Little NA, Xirodimas DP, Frenk R, van der Eb AJ, Lane DP, Saville MK, Jochemsen AG. Mdmx stabilizes p53 and Mdm2 via two distinct mechanisms. EMBO Rep 2001; 2:1029-34.
24. Li M, Brooks CL, Kon N, Gu W. A dynamic role of HAUSP in the p53-Mdm2 pathway. Mol Cell 2004; 13:879-86.
25. Grossman SR, Deato ME, Brignone C, Chan HM, Kung AL, Tagami H, Nakatani Y, Livingston DM. Polyubiquitination of p53 by a ubiquitin ligase activity of p300. Science 2003; 300:342-4.
26. Goldbeter A, Koshland Jr DE. An amplified sensitivity arising from covalent modification in biological systems. Proc Natl Acad Sci USA 1981; 78:6840-4.
27. Stommel JM, Wahl GM. Accelerated MDM2 auto-degradation induced by DNA-damage kinases is required for p53 activation. Embo J 2004; 23:1547-56.
28. Meulmeester E, Pereg Y, Shiloh Y, Jochemsen AG. ATM-mediated phosphorylations inhibit Mdmx/Mdm2 stabilization by HAUSP in favor of p53 activation. Cell Cycle 2005; 4:1166-70.
29. Stommel JM, Wahl GM. A new twist in the feedback loop: Stress-activated MDM2 destabilization is required for p53 activation. Cell Cycle 2005; 4:411-7.
30. Yin Y, Stephen CW, Luciani MG, Fahraeus R. p53 Stability and activity is regulated by Mdm2-mediated induction of alternative p53 translation products. Nat Cell Biol 2002; 4:462-7.
31. Meek DW. Multisite phosphorylation and the integration of stress signals at p53. Cell Signal 1998; 10:159-66.
32. Meek DW, Milne DM. Analysis of multisite phosphorylation of the *p53* tumor-suppressor protein by tryptic phosphopeptide mapping. Methods Mol Biol 2000; 99:447-63.
33. Brooks CL, Gu W. Ubiquitination, phosphorylation and acetylation: The molecular basis for p53 regulation. Curr Opin Cell Biol 2003; 15:164-71.
34. Deguin-Chambon V, Vacher M, Jullien M, May E, Bourdon JC. Direct transactivation of *c-Ha-Ras* gene by *p53*: Evidence for its involvement in p53 transactivation activity and p53-mediated apoptosis. Oncogene 2000; 19:5831-41.
35. Kuznetsov YA. Elements of applied bifurcation theory. Springer 2004.
36. Shimada A, Kato S, Enjo K, Osada M, Ikawa Y, Kohno K, Obinata M, Kanamaru R, Ikawa S, Ishioka C. The transcriptional activities of p53 and its homologue p51/p63: Similarities and differences. Cancer Res 1999; 59:2781-6.
37. Calabro V, Mansueto G, Parisi T, Vivo M, Calogero RA, La Mantia G. The human MDM2 oncoprotein increases the transcriptional activity and the protein level of the p53 homolog p63. J Biol Chem 2002; 277:2674-81.
38. el-Deiry WS, Tokino T, Velculescu VE, Levy DB, Parsons R, Trent JM, Lin D, Mercer WE, Kinzler KW, Vogelstein B. WAF1, a potential mediator of *p53* tumor suppression. Cell 1993; 75:817-25.
39. Fiscella M, Zhang H, Fan S, Sakaguchi K, Shen S, Mercer WE, Vande Woude GF, O'Connor PM, Appella E. Wip1, a novel human protein phosphatase that is induced in response to ionizing radiation in a p53-dependent manner. Proc Natl Acad Sci USA 1997; 94:6048-53.
40. Li M, Zhou JY, Ge Y, Matherly LH, Wu GS. The phosphatase MKP1 is a transcriptional target of p53 involved in cell cycle regulation. J Biol Chem 2003; 278:41059-68.
41. Moroni MC, Hickman ES, Lazzerini Denchi E, Caprara G, Colli E, Cecconi F, Muller H, Helin K. Apaf-1 is a transcriptional target for E2F and p53. Nat Cell Biol 2001; 3:552-8.
42. Nakano K, Vousden KH. PUMA, a novel proapoptotic gene, is induced by *p53*. Mol Cell 2001; 7:683-94.
43. Oda K, Arakawa H, Tanaka T, Matsuda K, Tanikawa C, Mori T, Nishimori H, Tamai K, Tokino T, Nakamura Y, Taya Y. p53AIP1, a potential mediator of p53-dependent apoptosis, and its regulation by Ser-46-phosphorylated p53. Cell 2000; 102:849-62.
44. Okamura S, Arakawa H, Tanaka T, Nakanishi H, Ng CC, Taya Y, Monden M, Nakamura Y. *p53DINP1*, a p53-inducible gene, regulates p53-dependent apoptosis. Mol Cell 2001; 8:85-94.
45. Ueda K, Arakawa H, Nakamura Y. Dual-specificity phosphatase 5 (DUSP5) as a direct transcriptional target of tumor suppressor p53. Oncogene 2003; 22:5586-91.
46. Yin Y, Liu YX, Jin YJ, Hall EJ, Barrett JC. PAC1 phosphatase is a transcription target of p53 in signalling apoptosis and growth suppression. Nature 2003; 422:527-31.
47. Yu J, Zhang L. No PUMA, no death: Implications for p53-dependent apoptosis. Cancer Cell 2003; 4:248-9.
48. Bode AM, Dong Z. Post-translational modification of *p53* in tumorigenesis. Nat Rev Cancer 2004; 4:793-805.
49. Meek DW. Post-translational modification of p53. SeminCancer Biol 1994; 5:203-10.
50. Meek DW. Post-translational modification of p53 and the integration of stress signals. PatholBiol (Paris) 1997; 45:804-14.
51. Ferraro E, Corvaro M, Cecconi F. Physiological and pathological roles of Apaf1 and the apoptosome. J Cell Mol Med 2003; 7:21-34.
52. Robles AI, Bemmels NA, Foraker AB, Harris CC. APAF-1 is a transcriptional target of p53 in DNA damage-induced apoptosis. Cancer Res 2001; 61:6660-4.
53. Furukawa Y, Nishimura N, Furukawa Y, Satoh M, Endo H, Iwase S, Yamada H, Matsuda M, Kano Y, Nakamura M. Apaf-1 is a mediator of E2F-1-induced apoptosis. J Biol Chem 2002; 277:39760-8.
54. Bulavin DV, Demidov ON, Saito S, Kauraniemi P, Phillips C, Amundson SA, Ambrosino C, Sauter G, Nebreda AR, Anderson CW, Kallioniemi A, Fornace Jr AJ, Appella E. Amplification of PPM1D in human tumors abrogates *p53* tumor-suppressor activity. Nat Genet 2002; 31:210-5.
55. Harper JW, Elledge SJ, Keyomarsi K, Dynlacht B, Tsai LH, Zhang P, Dobrowolski S, Bai C, Connell-Crowley L, Swindell E. Inhibition of cyclin-dependent kinases by p21. Mol Biol Cell 1995; 6:387-400.
56. Harris SL, Levine AJ. The p53 pathway: Positive and negative feedback loops. Oncogene 2005; 24:2899-908.
57. Tyson JJ. Monitoring p53's pulse. Nat Genet 2004; 36:113-4.
58. Tyson JJ. Another turn for p53. 2006, (in press).
59. Sha W, Moore J, Chen K, Lassaletta AD, Yi CS, Tyson JJ, Sible JC. Hysteresis drives cell-cycle transitions in *Xenopus* laevis egg extracts. Proc Natl Acad Sci USA 2003; 100:975-80.
60. Wagner J, Ma L, Rice JJ, Hu W, Levine AJ, Stolovitzky GA. p53—Mdm2 loop controlled by a balance of its feedback strength and effective dampening using ATM and delayed feedback. IEE Proceedings - Systems Biology 2005; 152:109-18.
61. Lupardus PJ, Cimprich KA. Checkpoint adaptation; molecular mechanisms uncovered. Cell 2004; 117:555-6.
62. Kohn KW, Pommier Y. Molecular interaction map of the p53 and Mdm2 logic elements, which control the Off-On switch of p53 in response to DNA damage. Biochem Biophys Res Commun 2005; 331:816-27.
63. Fridman JS, Lowe SW. Control of apoptosis by p53. Oncogene 2003; 22:9030-40.
64. Chipuk JE, Bouchier-Hayes L, Kuwana T, Newmeyer DD, Green DR. PUMA couples the nuclear and cytoplasmic proapoptotic function of p53. Science 2005; 309:1732-5.
65. Hu MC, Qiu WR, Wang YP. JNK1, JNK2 and JNK3 are p53 N-terminal serine 34 kinases. Oncogene 1997; 15:2277-87.
66. Milne DM, Campbell DG, Caudwell FB, Meek DW. Phosphorylation of the tumor suppressor protein p53 by mitogen-activated protein kinases. J Biol Chem 1994; 269:9253-60.
67. Bissonnette N, Hunting DJ. p21-induced cycle arrest in G_1 protects cells from apoptosis induced by UV-irradiation or RNA polymerase II blockage. Oncogene 1998; 16:3461-9.
68. Li J, Yang Y, Peng Y, Austin RJ, van Eyndhoven WG, Nguyen KC, Gabriele T, McCurrach ME, Marks JR, Hoey T, Lowe SW, Powers S. Oncogenic properties of PPM1D located within a breast cancer amplification epicenter at 17q23. Nat Genet 2002; 31:133-4.
69. Bernards R. Wip-ing out cancer. Nat Genet 2004; 36:319-20.